JACS
JOURNAL OF THE AMERICAN CHEMICAL SOCIETY

Article

pubs.acs.org/JACS

Electrostatically Guided Dynamics—The Root of Fidelity in a Promiscuous Terpene Synthase?

Dan Thomas Major* and Michal Weitman

Department of Chemistry and the Lise Meitner-Minerva Center of Computational Quantum Chemistry, Bar-Ilan University, Ramat-Gan 52900, Israel

Supporting Information

ABSTRACT: Terpene cyclases are responsible for the initial cyclization cascade in the multistep synthesis of more than 60 000 known natural products. This abundance of compounds is generated using a very limited pool of substrates based on linear isoprenoids. The astounding chemodiversity obtained by terpene cyclases suggests a tremendous catalytic challenge to these often promiscuous enzymes. In the current study we present a detailed mechanistic view of the biosynthesis of the monoterpene bornyl diphosphate (BPP) from geranyl diphosphate by BPP synthase using state of the art simulation methods. We identify the bornyl cation as an enzyme-induced bifurcation point on the multidimensional free energy surface, connecting between the product BPP and the side product camphene. Chemical dynamics simulations suggest that the active site diphosphate moiety steers reaction trajectories toward product formation. Nonetheless, chemical dynamics is not precise enough for exclusive product formation, providing a rationale for the lack of fidelity in this promiscuous terpene cyclase.

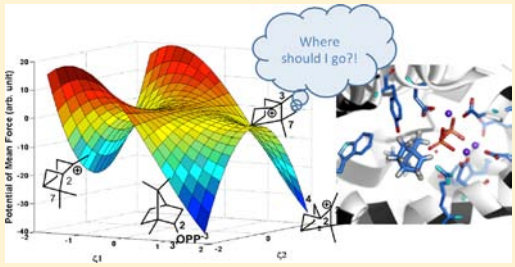

INTRODUCTION

Enzymes catalyze chemical reactions in the cells of all organisms in nature.[1] In the absence of enzymes, life as we know it would not be possible. These biocatalysts enhance the rate of chemical reactions to values approaching the diffusion limit of bimolecular encounters in water.[2] Decades of comparisons between enzymatic reaction rates and their nonenzymatic counterparts have revealed astonishing rate enhancements of up to 10^{17}-fold.[3,4] No less intriguing than the rate enhancement is the narrow range of observed rate constants in enzymes compared to the much wider range seen in nonenzymatic reactions. Indeed, the spread in reaction rate values in enzymes is 10 orders of magnitude smaller, suggesting that enzymes have evolved to produce chemical rates compatible with a rather uniform time scale of cellular processes.[1]

To achieve such catalytic perfection, enzymes employ numerous physicochemical tools with the ultimate goal of reducing the free energy barrier. A widely accepted mechanism for free energy barrier reduction in enzymes is a preferential stabilization of the transition state (TS)[5] in enzymes compared to that of an equivalent reaction in water.[4] This in turn may be associated with the considerably greater cost of solvent reorganizing in moving from the reactant state (RS) to the TS in the nonenzymatic reaction compared to that in the enzyme reaction, where the active site is preorganized.[6] Numerous additional catalytic effects—such as RS destabilization, desolvation,[7] covalent bonding,[8] quantum mechanical tunneling,[9,10] and enzyme dynamics[11,12]—have been suggested.

Interestingly, in the generation of many natural compounds, the principle catalytic challenge seems to be reaction control and precision rather than rate enhancement.[13] In the biosynthesis of natural compounds, a limited stock of simple metabolites is employed to generate exquisite chemodiversity.[14] For example, terpenoids (isoprenoids) form a large family of structurally and stereochemically diverse natural compounds[15−23] with only modest rate enhancements.[24−26] Despite this limited rate enhancement, there is no questioning the immense synthetic challenge facing terpene cyclases.[15,16,18,21,27]

Currently, more than 60 000 isoprenoids have been identified, and their chemistry has been studied comprehensively by experimental methods.[14,16,18,28] Cyclic terpenoid compounds are formed via complex carbocation cyclization reactions involving highly reactive carbocation intermediates that must be sequestered within the active site to avoid abortive side reactions.[16] Due to the transient nature of carbocations, however, the presence of many intermediate structures is merely postulated. Additionally, an active role of bound diphosphate during catalysis has been proposed by numerous researchers.[29−32] Extensive theoretical studies have addressed mechanistic aspects of terpene carbocation reactions, both in the gas phase[33] and in enzymes.[34−36]

The simplest form of terpenoid chemistry is found for monoterpenes, which give plants fragrance, flavor, and medicinal properties[23,37,38] and which have also been suggested as important players in organic aerosol formation.[39] An extensively studied monoterpene cyclase is (+)-bornyl diphosphate synthase (BPPS).[18] The crystal structure of

Received: August 21, 2012
Published: October 29, 2012

   dx.doi.org/10.1021/ja308295p | J. Am. Chem. Soc. 2012, 134, 19454−19462

Scheme 1. (a) Geranyl Diphosphate Cyclization to Bornyl Diphosphate Catalyzed by BPPS and (b) Possible Carbocation Intermediates in the Cyclization of Geranyl Diphosphate to Bornyl Diphosphate by BPPS

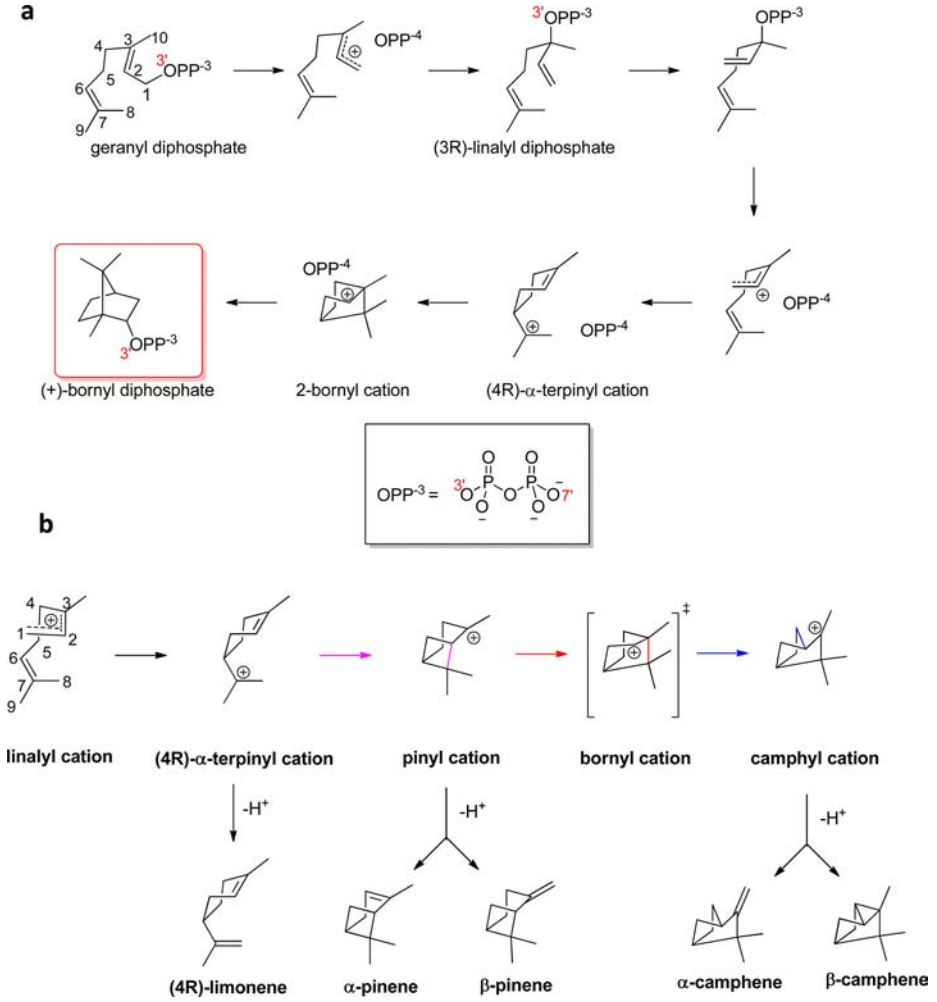

BPPS was solved in the presence of several ligands representing intermediate states of the proposed reaction, including a product mimic of (+)-bornyl diphosphate (BPP).[40] An essential active site water molecule was also identified. These crystal structures provide information on the main steps in the reaction cascade, some of which are presented in Scheme 1a. The final product, BPP, is formed in ca. 75% yield.[41] This putative mechanism has received accruing support from experiments[40−48] with isotopic labeled substrates[42,43,45,48] as well as substrate and intermediate analogues.[40] In addition to the main product BPP, the promiscuous BPPS also produces significant amounts of (+)-α-pinene, (+)-camphene, (±)-limonene, and terpinolene, with (+)-camphene being the main side product (Scheme 1b).[41,47]

Computational gas-phase studies suggest numerous possible side reactions for BPPS (Scheme 1b).[36,49] The possible side reactions include migrations, hydride transfers, proton transfers, or deprotonations, which could yield additional products such as limonene, terpinolene, camphene, α-pinene, β-pinene, β-phellandrene, α/β/γ/δ-terpinene, α-thijuene, sabinene, and 3-carene. Puzzlingly, many of the carbocations investigated are significantly more stable than the bornyl cation (Scheme 1a) in the gas phase and are formed through low energy barrier processes, further underscoring the BPPS product formation conundrum.[36,49] Moreover, we have suggested that the bornyl cation may constitute a bifurcation point on the gas-phase potential energy surface (PES).[36] Bifurcations occur in cases of two sequential TSs with no intervening energy minimum, and in systems possessing such a PES, reaction selectivity is determined by the shape of the PES and dynamic effects.[50,51] The central questions of the bifurcating nature of the bornyl cation in the presence of enzyme, the product distribution in BPPS, and the catalytic mechanism remain obscure, even for this seemingly simple terpene cyclase. In an attempt to elucidate these questions, we scrutinize the reaction mechanism in BPPS, using hybrid quantum mechanics−molecular mechanics (QM/MM)[52−54] simulations in conjunction with multidimensional free energy simulations and activated molecular dynamics (MD) simulations.

RESULTS

Bornyl Diphosphate Synthase Reaction Mechanism. The reaction mechanism in BPPS was studied using multidimensional free energy simulations as described in the Methods section. The current simulations commence with the (3*R*)-linalyl diphosphate (LPP) bound in the active site of BPPS. In this starting conformation, the C1−C2 bond is oriented in a position conducive to C1−C6 bond formation of the terpinyl cation in the *R*-configuration (fourth step in Scheme 1a). The initiation step of the carbocation cyclization

dx.doi.org/10.1021/ja308295p | J. Am. Chem. Soc. 2012, 134, 19454−19462

cascade is the dissociation of the C3−O3 bond, yielding a diphosphate−allyl cation ion pair. In Figure 1 we present the

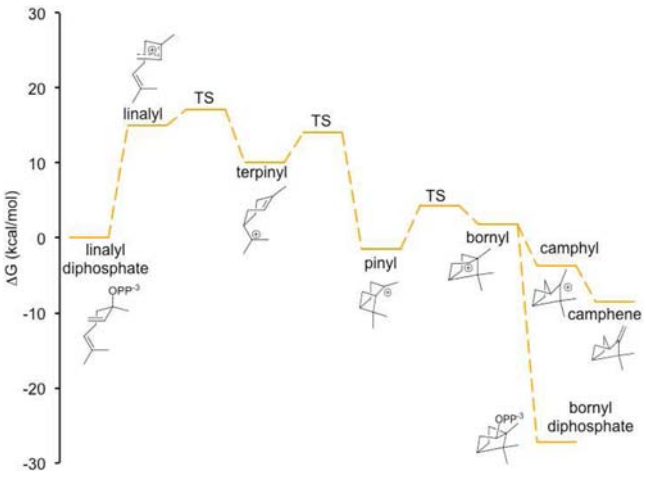

Figure 1. Free energy profile (kcal/mol) for the BPPS-catalyzed LPP to BPP reaction.

combined free energy profile for BPPS and in Figure S1 (Supporting Information) the free energy as a function of the C1−O3 and C3−O3 bond distances. Inspection of this free energy surface suggests that the computed free energy barrier is ca. 15 kcal/mol. This may be compared with a limiting value of 19.1 kcal/mol for 3*S*-LPP in limonene synthase, based on the experimental k_{cat} value.[26] We note that the isomerization of geranyl diphosphate (GPP) to LPP is assumed to be the rate-limiting chemical step.[43] The bond dissociation process reaches a plateau at C1−O3 and C3−O3 distances of ca. 3.0 Å, where the reactive linalyl cation species is stabilized by electrostatic interactions with the PP moiety (Figure S1, Supporting Information). We note that further distancing of the linalyl cation from the diphosphate moiety is largely avoided by a slightly higher free energy barrier (18.0 kcal/mol). This barrier is seemingly essential since further distancing of the linalyl cation would facilitate the formation of the terpinyl cation in a nonproductive conformation, as has been observed in the BPPS crystal structures.[40] Similar binding modes have been observed for bisabolyl carbocation mimics in trichodiene synthase as well.[55] Such nonproductive conformations could potentially yield unwanted side reactions such as premature deprotonation at C8 or C9 to yield (±)-limonene (Scheme 1b).

Following the formation of a linalyl cation, a terpinyl cation is formed through a low-barrier process with $\Delta G^{\ddagger}$ = 2.1 kcal/mol (Figures 1 and S2 and S4, Supporting Information). The reaction free energy for this step is −5.0 kcal/mol. This may be compared to a value of −15.2 kcal/mol in the gas phase (Table S1, Supporting Information). A likely reason for the less favorable process in the enzyme is the migration of the positive charge from near proximity to the pyrophosphate moiety in the initial ion pair to a position buried in the hydrophobic part of the active site (Table S2, Supporting Information). Attempts to form a terpinyl cation directly from (3*R*)-LPP in a concerted, synchronous step resulted in a very high free energy barrier (results not shown), and we conclude that full dissociation of the linalyl cation from the diphosphate group to form the ion pair is required prior to the terpinyl carbocation formation. This is in agreement with the experimental assessment that a distinct ion pair exists.[43,45] We may thus define the transformation (3R)-LPP → terpinyl cation as concerted-asynchronous.[56]

Subsequently, the terpinyl cation is expected to form a bornyl cation (Scheme 1) although gas-phase calculations suggest pinyl cation formation.[36] To quantitatively probe the formation of pinyl and bornyl cations from the terpinyl cation, we performed further multidimensional umbrella sampling simulations (Figure 2). Attempts to produce the bornyl cation

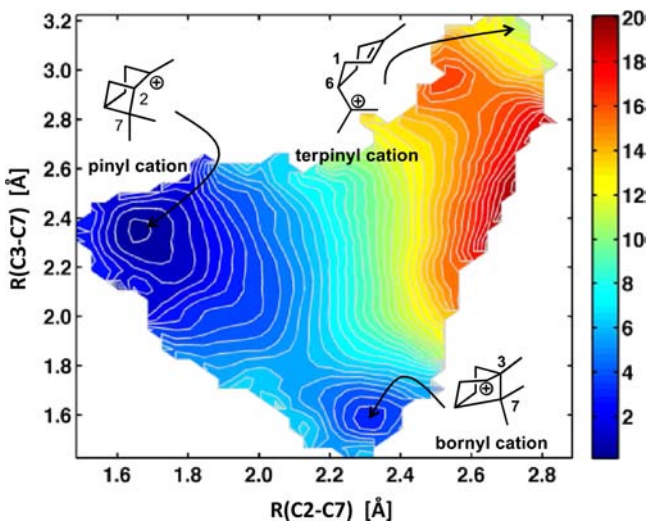

Figure 2. Two-dimensional slice of the multidimensional classical potential of mean force (kcal/mol) for the formation of the pinyl and the bornyl cations from the (4*R*)-α-terpinyl cation in BPPS. Contour levels correspond to 0.5 kcal/mol.

directly from the terpinyl cation (applying a biasing force to the C3−C7 bond) proceeded via a pinyl cation (Figure S5−S7, Supporting Information). This strongly suggests that the reaction mechanism in BPPS goes via a pinyl cation, as is the case in the gas phase.[36,49] Interestingly, this possibility was alluded to in the early work of Wise et al.[47] The free energy surface suggests a small initial barrier (4.0 kcal/mol) followed by the steepest descent path from the terpinyl to the pinyl cation. The free energy gain upon pinyl cation formation is −11.5 kcal/mol relative to the terpinyl cation. This may be compared to a gas-phase value of −5.5 kcal/mol (Table S1, Supporting Information). The driving force for this step is seemingly a combination of formation of a strained σ-bond and the charge migration during the ring closure (Table S2, Supporting Information). The short lifetime of the terpinyl carbocation is likely crucial to avoid unwanted hydride and proton transfers.[36] Subsequently, the required bornyl cation may be formed from the pinyl cation via a free energy barrier of 5.8 kcal/mol (Figures 2, 3, and S5−S7, Supporting Information). The bornyl cation is destabilized by +3.3 kcal/mol relative to the pinyl cation (Figure 2). The barrier between the pinyl and the bornyl cations is induced by the enzyme environment—in the gas phase there is no barrier for the pinyl → bornyl endergonic transformation. The relative energy difference between the pinyl cation and the less stable bornyl cation in the gas phase is 9.2 kcal/mol (Table S1, Supporting Information). Considering the stability of the pinyl cation, potential side reactions could occur prior to the formation of the bornyl cation, such as the formation of pinene or fenchane.[36]

dx.doi.org/10.1021/ja308295p | J. Am. Chem. Soc. 2012, 134, 19454−19462

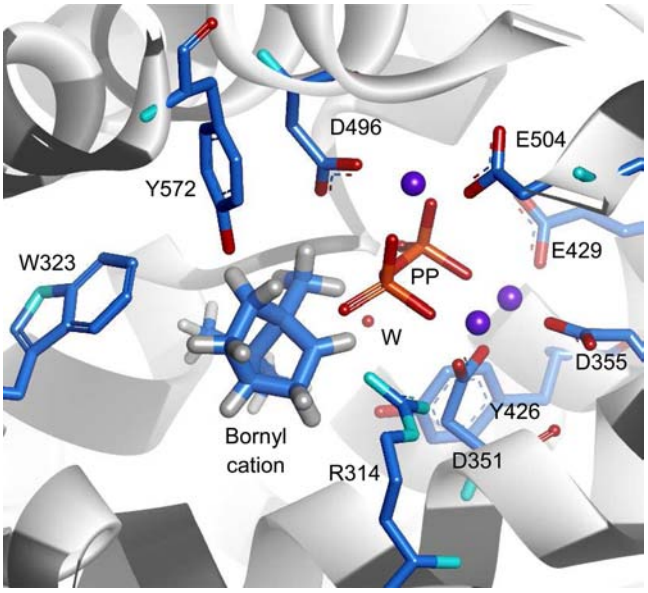

Figure 3. Snapshot of the bornyl cation in the active site of BPPS obtained from hybrid QM(M06-2X)/MM molecular dynamics simulations. Magnesium ions are shown in purple. Hydrophobic residues have dark-shaded ribbons, while hydrophilic residues have light-shaded ribbons.

Initial MD simulations of BPPS suggested that the bornyl cation (Figure 3) may be captured by the diphosphate moiety (Figure S8, Supporting Information) or rearranged to yield a camphyl cation (Figure S9, Supporting Information).[36] In principle, additional rearranged side products are also possible. To investigate these possible mechanistic pathways, we computed the free energy surface as a function of the bornyl → camphyl cation rearrangement coordinate and the C2−O3 bond distance (Figures 1 and 4). On the basis of this free energy map (Figure 4), we conclude that the bornyl cation is a transient species in the enzyme. Indeed, it is expected to rapidly form either the desired product BPP or camphyl cation en route to the side product camphene. The product BPP is strongly favored thermodynamically, with a reaction free energy of −29.0 kcal/mol. Additionally, the bornyl cation is perfectly oriented to form the (+)-BPP enantiomer, and we see no formation of the (−)-BPP enantiomer, in agreement with experiment.[47] In comparison, the formation of a camphyl cation yields −5.5 kcal/mol stabilization relative to the bornyl cation. In the gas phase, the camphyl cation is more stable than the bornyl cation by 19.4 kcal/mol (Table S1, Supporting Information). We note that once formed in the enzyme, the camphyl cation may produce camphene via deprotonation at the C3 exocyclic position or at C4 by PP or the active site water molecule (vide infra). Free energy simulations of camphyl deprotonation suggest that this proceeds via the active site water molecule, which is well-positioned to perform antiperiplanar proton abstraction (Figure 5). This camphyl deprotonation is accompanied by a concerted water proton transfer to the diphosphate moiety. Formation of camphene and protonated disphosphate is favored thermodynamically (−4.8 kcal/mol), and the barrier for such a process is less than 4 kcal/mol (including nuclear QM effects). Thus, once a camphyl cation is formed, it is rapidly deprotonated to form camphene. We note that BPP may be formed via reprotonation of camphene with a barrier of 10.3 kcal/mol, although deprotonation of the diphosphate moiety by nearby water molecules is a more likely scenario.

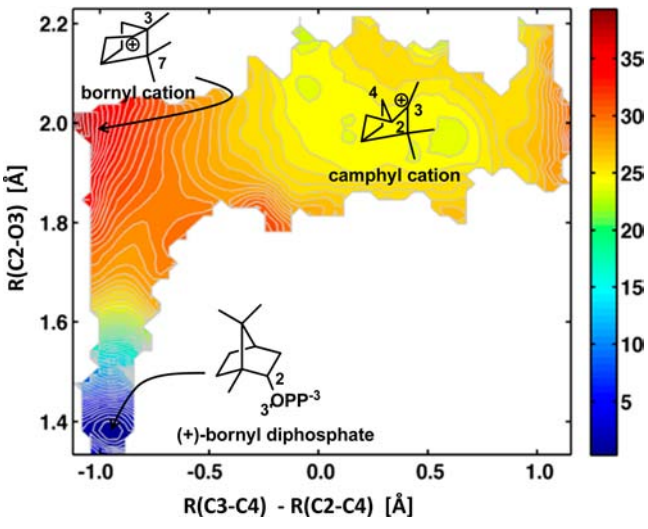

Figure 4. Two-dimensional slice of the multidimensional classical potential of mean force (kcal/mol) for the formation of BPP or the camphyl cation from the bornyl cation in BPPS. Contour levels correspond to 0.5 kcal/mol.

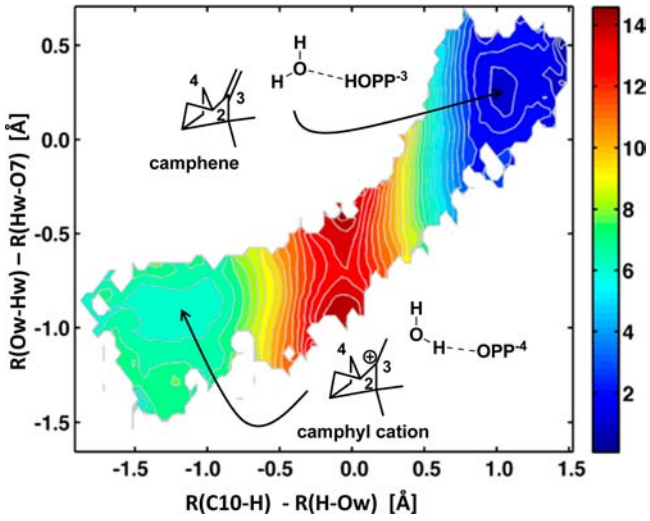

Figure 5. Two-dimensional classical potential of mean force (kcal/mol) for the deprotonation of the camphyl cation by an active site water molecule and diphosphate moiety. Contour levels correspond to 0.5 kcal/mol.

Dynamic Effects in the Bornyl Diphosphate Synthase Reaction. A key question is the exact nature of the bornyl cation (Figure 3) and what determines its fate. In our previous combined gas-phase and initial enzymatic study of the BPPS-catalyzed reaction we suggested that the bornyl cation is not a stable intermediate but rather a short-lived species.[36] Additionally, we suggested that the bornyl cation constituted a bifurcation point on the gas-phase potential energy surface. On the basis of our current results, it seems that this bifurcating nature is retained in the enzyme (Figure 6). We note that in the enzyme the principle bifurcation is between different species than in the gas phase. The bornyl cation is formed via a TS from the pinyl cation, whereupon bornyl descends directly onto another TS that separates the camphyl cation, and hence

dx.doi.org/10.1021/ja308295p | J. Am. Chem. Soc. 2012, 134, 19454−19462

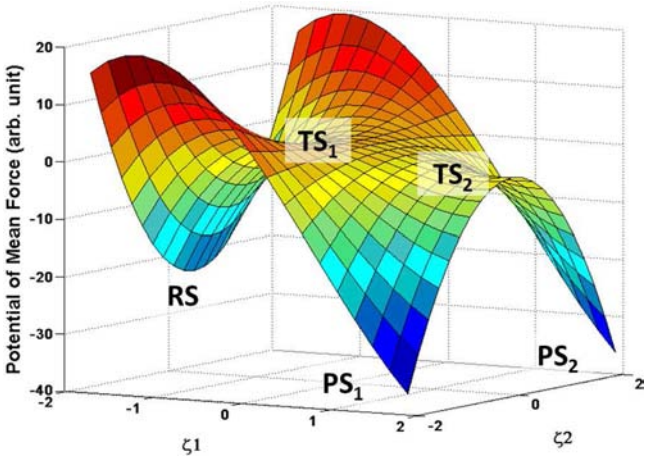

Figure 6. Schematic depiction of the bifurcating potential of mean force surface in BPPS. RS represents the pinyl cation and TS_1 the transition state between the pinyl cation and the bornyl cation (TS_2), while PS_1 and PS_2 represent bornyl diphosphate and camphene, respectively.

camphene, and BPP (Figures 1, 4–6). In such a bifurcating case, the branching ratio between camphene and BPP is determined by chemical dynamics. To probe the question of the dynamics of branching of the bornyl carbocation to BPP and camphene, we performed activated dynamics simulations.[57] Interestingly, related branching points were alluded to by Hong and Tantillo based on calculations on model systems.[49]

An ensemble of forward trajectories was initiated from the kinetic bottleneck separating the pinyl and the bornyl cations. The dividing surface was defined as R(C2–C7) = 2.10 ± 0.02 Å and R(C3–C7) = 1.80 ± 0.02 Å (Figures 2 and S6, Supporting Information). At the pinyl → bornyl cation TS, shown schematically as TS_1 in Figure 6, the ensemble averaged C2–O3 distance is 2.8 ± 0.1 Å. Commencing from this point, we propagated 50 trajectories in the direction of the bornyl cation (for details, see the Methods section). The trajectories are presented in Figure 7a, and in all cases a camphyl cation or BPP is formed within a few hundred femtoseconds, suggesting that bornyl cation is a short-lived species in BPPS. We also note that the bornyl cation is a required intermediate, and formation of BPP and camphene always passes through this cation (Figure S10, Supporting Information). Moreover, once a product is formed it remains stable for the remainder of the simulation. Inspection of the trajectories suggests a clear preference for BPP formation over camphyl cation formation. The product distribution is presented in Figure 7b and shows a 1:0.1 ratio of BPP:camphyl formation, in agreement with experiment.[41,47] We note that initiating MD trajectories with the bornyl cation, i.e., at the TS separating BPP and the camphyl cation (Figure 4 and TS_2 in Figure 6), does not yield a preference for BPP formation (Figure 8). Indeed, 75 MD trajectories initiated with the bornyl cation [R(C3–C7) ≈ 1.6 Å] yield a nearly equal BPP:camphyl distribution (see Supporting Information for further information). BPP is preferentially obtained when the simulations are initiated at shorter C2–O3 ion pair distances, while at longer distances rearrangement to a camphyl cation is observed. This suggests that the active mode at the preceding TS (TS_1 in Figure 6) is essential in directing the reaction flux toward BPP formation. Indeed, had dynamic effects not been in play, we should have expected a Maxwell–Boltzmann distribution of velocities in the bornyl cation state. Our

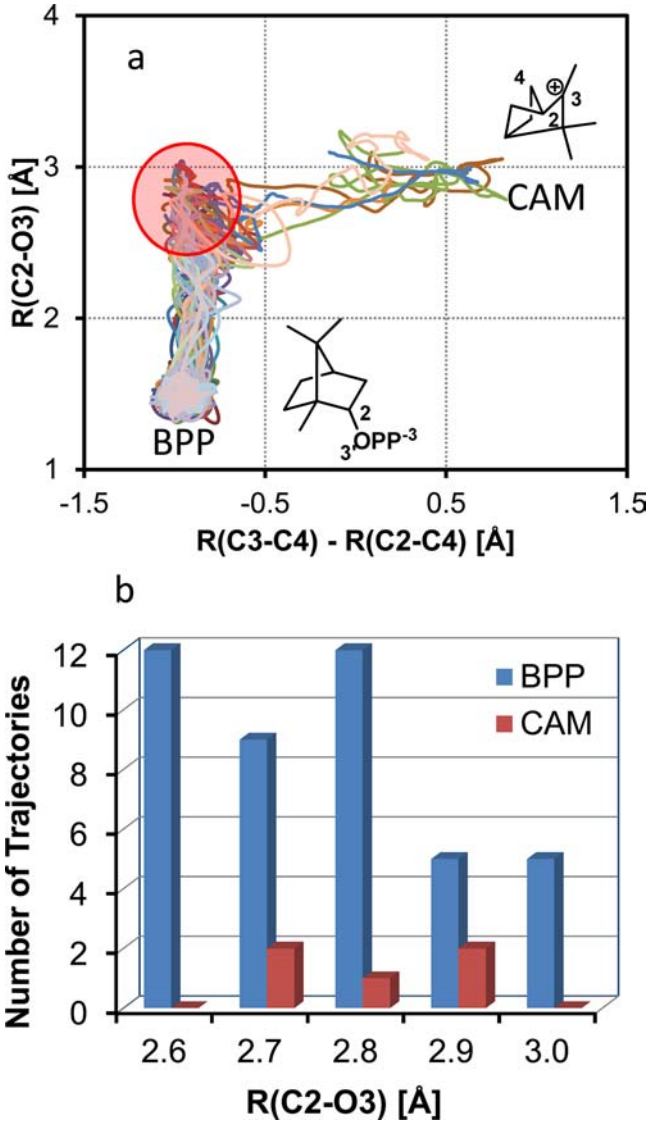

Figure 7. Activated classical molecular dynamics trajectories for the formation of BPP or the camphyl cation (CAM) in BPPS. The forward trajectories were initiated at the dividing surface between the pinyl and the bornyl cations at various distances from the diphosphate group. (a) Trajectories initiated in the encircled region and ending either with BPP or CAM. (b) Distribution of products as a function of initial distance from pyrophosphate moiety.

activated dynamics simulations initiated with the bornyl cation (TS_2 in Figure 6) model such a scenario, and as stated no preferential BPP formation is observed, in contradiction with experiment. A related analysis has been performed by Warshel and Chu in the study of surface crossing in bacteriorhodopsin, where inertial and overdamped models were employed to determine the nature of the photochemical event.[58]

■ DISCUSSION

We may now address the key questions on BPPS catalysis, namely, how bornyl diphosphate is formed in spite of the significant catalytic challenges and how do we account for the experimentally observed side products limonene, pinene, and camphene. On the basis of the current results, we would expect BPP to be the major product, as is observed experimentally.[41,47] The formation of BPP is strongly favored thermodynamically

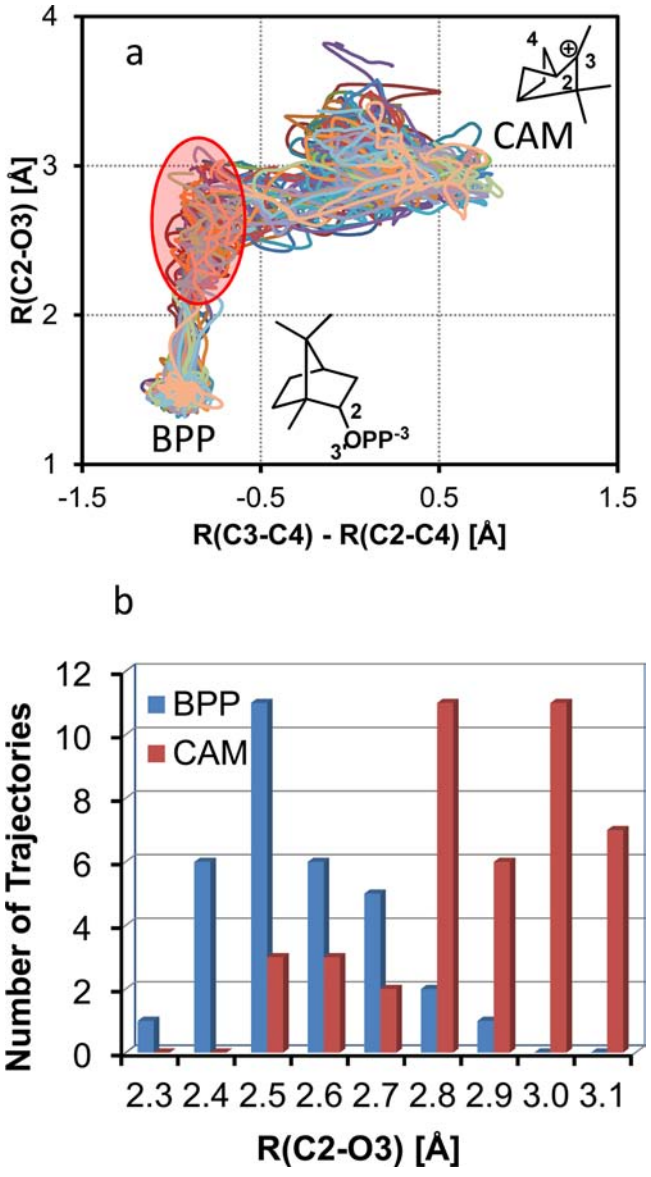

Figure 8. Activated classical molecular dynamics trajectories for the formation of BPP or the camphyl cation (CAM) in BPPS. The trajectories were initiated with the bornyl cation at various distances from the diphosphate group. (a) Trajectories initiated in the encircled region and ending either with BPP or CAM. (b) Distribution of products as a function of initial distance from pyrophosphate moiety.

and, once formed, no reverse reaction is possible. However, the reaction path to BPP is prone to chemical errors. In the absence of an enzyme, the carbocation bornyl forms exclusively the camphyl cation,[36] and even in the enzyme it is a transient molecule. Truly, the bornyl cation constitutes a branching point, and the enzyme needs to funnel the reaction from the terpinyl cation, via a pinyl cation, toward the desired product BPP and away from camphene formation. The current simulations suggest that this is achieved by electrostatic guidance and dynamical effects, as will be detailed below.

In order for BPPS to yield selectivity, electrostatics is employed as a guiding force en-route to the final product. The initial binding of the substrate is such that the general fold is conducive to correct cyclization.[40] Following heterolytic cleavage of (3*R*)-linalyl diphosphate, the linalyl cation is precisely positioned for subsequent formation of a terpinyl cation, presumably via electrostatic interactions. The terpinyl cation is formed via a low barrier, concerted, asynchronous process, yielding what is seemingly not the global free energy minimum in BPPS,[40] since the cation at the C7 position (Scheme 1 and Figure S4, Table S2, Supporting Information) is not in immediate proximity to the diphosphate group. However, this intermediate is short-lived and rapidly forms a pinyl cation with the positive charge at the C3 position in close vicinity of the diphosphate (Figure S5 and Table S2, Supporting Information). The electrostatic interactions orient the intermediate in a manner that likely minimizes the possibility for side reactions and enables the formation of the bornyl cation via a low-barrier process (Figures 2 and 3 and S7, Supporting Information). Subsequently, electrostatic effects ensure that the bornyl cation enjoys direct ion-pair stabilization (Figure S7, Table S2, Supporting Information). Indeed, the relative stability of the bornyl and the camphyl cations is significantly perturbed in the enzyme, compared to the gas phase, in favor of the bornyl cation. Seemingly, such a use of electrostatics is essential in the absence of any specific interactions between the carbocations and the protein matrix. Nonetheless, electrostatic interactions are seemingly insufficient to ensure committed product formation on a bifurcating potential of mean force surface, and dynamical effects are required. Indeed, product distribution in BPPS is not predictable on the basis of thermodynamics and kinetics alone. Rather, product formation is realized in the reaction flux that is funnelled toward BPP formation, as is evident from activated dynamics simulations and normal-mode analyses of the dividing surface ensemble separating between the pinyl and the bornyl cations (see the Methods section). Similar asymmetric funneling of product distribution has been suggested for photochemical processes in crystals.[59] The active mode that forms the bornyl cation includes coupled motions that combine rearrangement from the pinyl to the bornyl cation [i.e., the antisymmetric stretch coordinate R(C2−C7)−R(C3−C7)] as well as compression of the C2−O3 distance, assisting BPP formation (see the movie in Supporting Information). To the best of our knowledge such dynamical effects have not previously been observed in enzymes,[60] although Villà and Warshel hinted that such effects may exist in systems with low-barrier processes.[61] Here we suggest that dynamic effects may play a crucial role in terpene cyclases, which are enzymes with highly complex potential energy surfaces with a multitude of stationary points separated by low barriers. We note that dynamical effects have been implicated in other terpenes on the basis of gas-phase calculations.[62,63]

On the basis of the current simulations, we may also readily understand the possible formation of limonene, pinene, or camphene (Scheme 1). A slight misfold of the initial substrate or enzyme, the tumbling of the intermediate during catalysis, or imprecise barrier crossings may allow abortive deprotonation to form side products. A likely deprotonating agent would be the diphosphate moiety (via the O3 or O7 atoms) or the active site water molecule (OW atom) that hydrogen bonds directly to the diphosphate O7 atom. As shown herein, deprotonation of the camphyl cation by the active site water molecule and diphosphate, to yield camphene, is expected to be a rapid process. Protonation of the diphosphate moiety might subsequently trigger a product release process.

In summary, this work proposes a multilevel catalytic strategy in one of the simplest terpenes, BPPS. The potential of mean force surface in BPPS is highly complex, with transient species

separated by low free-energy barriers and a bifurcation point. In particular, BPPS employs the pyrophosphate moiety to guide the reaction toward product formation. However, in order to achieve chemical control on such an intricate free energy landscape, BPPS needs to employ dynamical effects to ensure primary formation of the product BPP. Herein is the root of its promiscuity: electrostatics and dynamics, in the absence of directional hydrogen bonds, are not sufficiently precise to achieve exclusive product formation, and as a result numerous side products are observed. Further studies of terpene cyclases employing more accurate potential energy surfaces, longer simulations, and additional theoretical frameworks in order to quantify the magnitude of the dynamical effect are expected to scrutinize the currently proposed role of dynamics.

CONCLUSION

In the current study we present a detailed mechanistic view of the biosynthesis of the monoterpene bornyl diphosphate (BPP) from geranyl diphosphate by BPP synthase (BPPS). We employ molecular dynamics and multidimensional free energy simulations on an accurate hybrid quantum mechanics−molecular mechanics potential energy surface to study the enzymatic pathways. We identify the bornyl cation as a key mechanistic branching point that can form the product BPP as well as the side product camphene. Initial heterolytic C−O bond cleavage in (3*R*)-linalyl diphosphate yields a linalyl cation, followed by formation of terpinyl and pinyl cations. Subsequently, the bornyl cation is formed via a low, enzyme-induced barrier separating the bornyl cation from the pinyl cation. Importantly, the bornyl cation is not a stable species but serves as a TS between BPP and the camphyl cation. The bornyl cation may be viewed as an enzyme-induced bifurcation point on the potential of mean force multidimensional surface. Chemical dynamics simulations suggest that a key factor in assuring BPP formation is electrostatic steering by the diphosphate moiety, which directs reaction trajectories toward product formation. Nonetheless, chemical dynamics is not precise enough for exclusive product formation, providing a long sought after rationale for the lack of fidelity in this promiscuous terpene cyclase. The current results suggest that terpene cyclases such as BPPS may have evolved to direct product distribution via dynamical effects, even though this is a possible reason for their promiscuity.

METHODS

Gas-Phase Modeling. We have previously performed extensive benchmark calculations of various DFT and high-level ab initio methods on small carbocation compounds in order to assess the most reliable functional for the study of terpenes in general and monoterpenes in particular. In the current study, we employ the M06-2X hybrid DFT approach[64] with a 6-31+G(d,p) basis set.[65] In Tables S1 and S2 (Supporting Information) we present gas-phase results for model carbocations and monoterpenes. The current results compare well with those obtained from high-level ab initio methods. All stationary points were characterized with frequency calculations, and a scaling factor of 0.967 was used for all frequencies.[66] All gas-phase calculations were performed with the Gaussian 09 program.[67]

Enzyme Modeling. The reaction mechanism in BPPS was addressed by several complementary strategies. Initially, unbiased MD simulations of key proposed intermediates were performed to probe the intrinsic reactivity of the species. Subsequently, the full enzyme reaction mechanism was studied with free energy simulations using adaptive multidimensional umbrella sampling simulations[68,69] and a recently developed multidimensional version of the weighted histogram analysis method (WHAM) code.[70] Finally, activated forward MD simulations were performed with trajectories initiated at different dividing surfaces in phase space, and the evolution of the trajectories was followed until they were quenched in product states.

Model of the Solvated Enzyme−Coenzyme−Substrate Complex. As described previously, the X-ray crystallography structure of dimeric (+)-bornyl diphosphate synthase from *Salvia officinalis*, published by Whittington et al. (PDB ID: 1N23),[40] was used as a starting point for the simulations.[36] The 2-azabornane in the active site was manually modified to the 2-bornyl cation, and the system was solvated with a 20 Å water sphere. The system was initially heated slowly to 298 K during the course of 25 ps and thereafter equilibrated for 75 ps. Subsequently, the system was further simulated for 1 ns. The current MD study employed stochastic boundary conditions for the enzymatic reaction due to the size of BPPS and the high cost of the QM/MM simulations.[71] Further details are provided in the Supporting Information.

Potential Energy Surface. The potential energy surface (PES) in the current study is described by a hybrid QM/MM Hamiltonian.[52] In this treatment, the reactive fragment wherein the chemistry occurs is treated via QM to allow for bond breaking and forming while the environmental effects of the enzyme and solvent are included via MM. The QM region contains the carbocation, diphosphate, and Mg^{2+} ions in one of the active sites and is described by the M06-2X functional[64] in conjunction with a hybrid basis set (see Supporting Information).[36] In simulations of deprotonation of the camphyl cation, the active site water was also treated as QM. The MM part is described by the CHARMM22 force field,[72] while water molecules are treated by the TIP3P model.[73] Further details are provided as Supporting Information.

Multidimensional Adaptive Umbrella Sampling Simulations. The current MD study employs stochastic boundary conditions for the enzymatic reaction due to the size of BPPS and the high cost of the QM/MM simulations.[71] The details of the MD simulations have been previously described.[36] The classical potential of mean force (PMF) as a function of the reaction coordinate was defined as

$$W^{\mathrm{cl}}(\zeta) = -RT \ln \rho(\zeta) + C \qquad (1)$$

where ρ is the unbiased probability density along a reaction coordinate ζ, R is the gas constant, T is the temperature, and C is an arbitrary constant.[57] In practice, we employed adaptive multidimensional umbrella sampling simulations[68,69] and a recently developed multi-dimensional version of the WHAM code.[70]

The reaction coordinates were defined by means of geometric variables relevant to different stages of the reaction mechanism (Scheme 1). We performed three separate sets of multidimensional adaptive umbrella sampling studies: (i) starting from (3*R*)-linalyl diphosphate and ending with terpinyl cation formation, (ii) starting from the terpinyl cation and ending with BPP or a camphyl cation. (iii) Deprotonation of the camphyl cation to yield camphene. In set i we defined three reaction coordinate variables: $\zeta_1 = R(\mathrm{C1-O3})$, $\zeta_2 = R(\mathrm{C3-O3})$, and $\zeta_3 = R(\mathrm{C1-C6})$. This set accounts for heterolytic cleavage of geranyl diphosphate and (3*R*)-linalyl diphosphate to yield the linalyl−diphosphate ion pair, as well as formation of the terpinyl cation. In set ii we defined four reaction coordinates: $\zeta_1 = R(\mathrm{C2-C7})$, $\zeta_2 = R(\mathrm{C3-C7})$, $\zeta_3 = R(\mathrm{C3-C4})-R(\mathrm{C2-C4})$, and $\zeta_4 = R(\mathrm{C2-O3})$. The former two coordinates in set ii represent formation of the pinyl and bornyl cations, respectively, from the terpinyl cation, whereas the latter two define the bornyl → camphyl cation migration and BPP formation, respectively. In set iii we defined two reaction coordinates, describing proton transfer from the camphyl cation to the active site water molecule and from water to the diphosphate moiety. Specifically, $\zeta_1 = R(\mathrm{C10-H})-R(\mathrm{H-O_W})$ and $\zeta_2 = R(\mathrm{O_W-H_W})-R(\mathrm{H_W-O7})$. The reaction coordinates were evenly spaced with 0.10−0.25 Å separation between centers of windows. Each window was briefly equilibrated for 2 ps and sampled for 5−10 ps each. The combined QM(M06-2X)/MM PMF simulation time was over 600 ps. Further details are provided as Supporting Information.

Normal Mode Analysis. To gain insight into the nature of the active mode at the TS separating the pinyl and bornyl cations, we performed normal-mode analysis for selected TS configurations. The Hessian matrix was computed numerically for the QM atoms only (i.e., in a fixed field of MM atoms).

Nuclear Quantum Effects. To account for zero-point vibrational energy and tunneling effects in the deprotonation of the camphyl cation, we used Monte Carlo path-integral simulations.[74] In the path-integral simulation approach, classical particles are replaced by a ring of quasiparticles (beads) to describe quantum delocalization. In the current study, we employ a recently developed high-order factorization of the thermal density matrix operator, which allows a significant reduction in the number of beads. Practically, we employed three beads per atom in conjunction with the staging sampling algorithm, as implemented in CHARMM.[74] Further details are provided as Supporting Information.

Activated Dynamics Simulations. Activated MD simulations[57] were performed by initiating trajectories from one of two initial states: (i) the bornyl cation region and (ii) the dividing surface between the pinyl and the bornyl cations (vide infra). The trajectories were followed for 0.5−1.0 ps, which was sufficient for the trajectory to quench in either the BPP or camphyl product well. In total, 125 such trajectories were run starting from different initial points in phase space, based on trajectory files from the umbrella sampling simulations. Of these trajectories, 50 were initiated at the transition state separating the pinyl and bornyl cations [R(C2−C7) = 2.10 ± 0.02 Å and R(C3−C7) = 1.80 ± 0.02 Å], while 75 of these were initiated from the bornyl cation [R(C3−C7) ≈ 1.6 Å and R(C2−O3) ≈ 2.5−3.0 Å]. The initial velocities of all atoms were randomized to give a Maxwell−Boltzmann distribution. For the reactive trajectories initiated at the TS between the pinyl and the bornyl cations, a forward filter was applied to generate exclusively reactive trajectories (i.e., discarding trajectories returning to the pinyl cation). The time step was 0.5 fs.

All QM(M06-2X)/MM simulations used the CHARMM simulation platform,[75,76] interfaced with the Q-CHEM program.[77]

■ ASSOCIATED CONTENT

Supporting Information

Additional free energy figures, figures of key structures during the BPPS catalytic cycle, tables of gas-phase calculation data and ensemble averaged structures from BPPS MD simulations, Cartesian coordinates of optimized gas-phase structures including absolute energies, and accompanying movies of key reaction steps. This material is available free of charge via the Internet at http://pubs.acs.org.

■ AUTHOR INFORMATION

Corresponding Author

majort@biu.ac.il

Notes

The authors declare no competing financial interest.

■ ACKNOWLEDGMENTS

This work has been supported by the Israel Science Foundation and the Minerva Stiftung. The authors thank Prof. A. Warshel and Prof. K. Nam for helpful comments on the manuscript.

■ REFERENCES

(1) Frey, P. A.; Hegeman, A. D. *Enzymatic Reaction Mechanisms*; Oxford University Press: New York, 2007.
(2) Alberty, R. A.; Hammes, G. G. *J. Phys. Chem.* **1958**, *62*, 154.
(3) Wolfenden, R. *Annu. Rev. Biochem.* **2011**, *80*, 645.
(4) Warshel, A.; Sharma, P. K.; Kato, M.; Xiang, Y.; Liu, H.; Olsson, M. H. M. *Chem. Rev.* **2006**, *106*, 3210.
(5) Pauling, L. *Am. Sci.* **1948**, *36*, 50.
(6) Yadav, A.; Jackson, R. M.; Holbrook, J. J.; Warshel, A. *J. Am. Chem. Soc.* **1991**, *113*, 4800.
(7) Gao, J.; Ma, S.; Major, D. T.; Nam, K.; Pu, J.; Truhlar, D. G. *Chem. Rev.* **2006**, *106*, 3188.
(8) Zhang, X.; Houk, K. N. *Acc. Chem. Res.* **2005**, *38*, 379.
(9) Major, D. T.; Heroux, A.; Orville, A. M.; Valley, M. P.; Fitzpatrick, P. F.; Gao, J. *Proc. Natl. Acad. Sci. U. S. A.* **2009**, *106*, 20734.
(10) Sen, A.; Kohen, A. *J. Phys. Org. Chem.* **2010**, *23*, 613.
(11) Glowacki, D. R.; Harvey, J. N.; Mulholland, A. J. *Nat. Chem.* **2012**, *4*, 169.
(12) Hay, S.; Scrutton, N. S. *Nat. Chem.* **2012**, *4*, 161.
(13) Clardy, J.; Walsh, C. *Nature* **2004**, *432*, 829.
(14) Gershenzon, J.; Dudareva, N. *Nat. Chem. Biol.* **2007**, *3*, 408.
(15) Croteau, R. *Chem. Rev.* **1987**, *87*, 929.
(16) Cane, D. E. *Chem. Rev.* **1990**, *90*, 1089.
(17) Lesburg, C. A.; Caruthers, J. M.; Paschall, C. M.; Christianson, D. W. *Curr. Opin. Struct. Biol.* **1998**, *8*, 695.
(18) Christianson, D. W. *Chem. Rev.* **2006**, *106*, 3412.
(19) Yoshikuni, Y.; Ferrin, T. E.; Keasling, J. D. *Nature* **2006**, *440*, 1078.
(20) Christianson, D. W. *Science* **2007**, *316*, 60.
(21) Allemann, R. K. *Pure Appl. Chem.* **2008**, *80*, 1791.
(22) Christianson, D. W. *Curr. Opin. Chem. Biol.* **2008**, *12*, 141.
(23) Degenhardt, J.; Kollner, T. G.; Gershenzon, J. *Phytochemistry* **2009**, *70*, 1621.
(24) Winstein, S.; Valkanas, G.; Wilcox, C. F. J. *J. Am. Chem. Soc.* **1972**, *94*, 2286.
(25) Cane, D. E.; Chiu, H. T.; Liang, P. H.; Anderson, K. S. *Biochemistry* **1997**, *36*, 8332.
(26) Williams, D. C.; McGarvey, D. J.; Katahira, E. J.; Croteau, R. *Biochemistry* **1998**, *37*, 12213.
(27) Xu, M.; Wilderman, P. R.; Peters, R. J. *Proc. Natl. Acad. Sci. U. S. A.* **2007**, *104*, 7397.
(28) Sacchettini, J. C.; Poulter, C. D. *Science* **1997**, *277*, 1788.
(29) Roy, A.; Roberts, F. G.; Wilderman, P. R.; Zhou, K.; Peters, R. J.; Coates, R. M. *J. Am. Chem. Soc.* **2007**, *129*, 12453.
(30) Greenhagen, B. T.; O'Maille, P. E.; Noel, J. P.; Chappell, J. *Proc. Natl. Acad. Sci. U. S. A.* **2006**, *103*, 9826.
(31) Shishova, E. Y.; Di Costanzo, L.; Cane, D. E.; Christianson, D. W. *Biochemistry* **2007**, *46*, 1941.
(32) Peters, R. J.; Croteau, R. B. *Arch. Biochem. Biophys.* **2003**, *417*, 203.
(33) Tantillo, D. J. *Nat. Prod. Rep.* **2011**, *28*, 1035.
(34) Rajamani, R.; Gao, J. *J. Am. Chem. Soc.* **2003**, *125*, 12768.
(35) Allemann, R. K.; Young, N. J.; Ma, S.; Truhlar, D. G.; Gao, J. *J. Am. Chem. Soc.* **2007**, *129*, 13008.
(36) Weitman, M.; Major, D. T. *J. Am. Chem. Soc.* **2010**, *132*, 6349.
(37) McCaskill, D.; Croteau, R. *Adv. Biochem. Eng. Biotechnol.* **1997**, *55*, 107.
(38) Davis, E. M.; Croteau, R. *Top. Curr. Chem.* **2000**, *209*, 53.
(39) Kiendler-Scharr, A.; Wildt, J.; Dal Maso, M.; Hohaus, T.; Kleist, E.; Mentel, T. F.; Tillmann, R.; Uerlings, R.; Schurr, U.; Wahner, A. *Nature* **2009**, *461*, 381.
(40) Whittington, D. A.; Wise, M. L.; Urbansky, M.; Coates, R. M.; Croteau, R. B.; Christianson, D. W. *Proc. Natl. Acad. Sci. U. S. A.* **2002**, *99*, 15375.
(41) Wise, M. L.; Savage, T. J.; Katahira, E.; Croteau, R. *J. Biol. Chem.* **1998**, *273*, 14891.
(42) Cane, D. E.; Saito, A.; Croteau, R.; Shaskus, J.; Felton, M. *J. Am. Chem. Soc.* **1982**, *104*, 5831.
(43) Croteau, R. B.; Shaskus, J. J.; Renstrøm, B.; Felton, N. M.; Cane, D. E.; Saito, A.; Chang, C. *Biochemistry* **1985**, *24*, 7077.
(44) Croteau, R.; Felton, M. *Arch. Biochem. Biophys.* **1981**, *207*, 460.
(45) Croteau, R.; Felton, N. M.; Wheeler, C. J. *J. Biol. Chem.* **1985**, *260*, 5956.
(46) Croteau, R.; Satterwhite, D. M.; Wheeler, C. J.; Felton, N. M. *J. Biol. Chem.* **1989**, *264*, 2075.

(47) Wise, M. L.; Pyun, H.-J.; Helms, G.; Assink, B.; Coates, R. M.; Croteau, R. B. *Tetrahedron* **2001**, *57*, 5327.
(48) Croteau, R.; Satterwhite, D. M.; Cane, D. E.; Chang, C. C. *J. Biol. Chem.* **1986**, *261*, 13438.
(49) Hong, Y. J.; Tantillo, D. J. *Org. Biomol. Chem.* **2010**, *8*, 4589.
(50) Ess, D. H.; Wheeler, S. E.; Iafe, R. G.; Xu, R.; Celebi-Olcum, N.; Houk, K. N. *Angew. Chem., Int. Ed.* **2008**, *47*, 7592.
(51) Hong, Y. J.; Tantillo, D. J. *Nat. Chem.* **2009**, *1*, 384.
(52) Warshel, A.; Levitt, M. *J. Mol. Biol.* **1976**, *103*, 227.
(53) Gao, J. *Methods and Applications of Combined Quantum Mechanical and Molecular Mechanical Potentials*; VCH: New York, 1995; Vol. 7.
(54) Senn, H. M.; Thiel, W. *Angew. Chem., Int. Ed.* **2009**, *48*, 1198.
(55) Vedula, L. S.; Rynkiewicz, M. J.; Pyun, H.-J.; Coates, R. M.; Cane, D. E.; Christianson, D. W. *Biochemistry* **2005**, *44*, 6153.
(56) Tantillo, D. J. *J. Phys. Org. Chem.* **2008**, *21*, 561.
(57) Northrup, S. H.; Pear, M. R.; Lee, C.-Y.; McCammon, J. A.; Karplus, M. *Proc. Natl. Acad. Sci. U. S. A.* **1982**, *79*, 4035.
(58) Warshel, A.; Chu, Z. T. *J. Phys. Chem. B* **2001**, *105*, 9857.
(59) Warshel, A.; Shakked, Z. *J. Am. Chem. Soc.* **1975**, *97*, 5679.
(60) The term "dynamical effects" used throughout this paper refer to nonequilibrium effects. This contrasts with the prevalent use of this term to describe conformational flexibility. The dynamical effects described herein arise due to the presence of bifurcation points on the potential of mean force surface. Such bifurcation points result in product distributions, which are not determined by relative free energies of competing transition states.
(61) Villa, J.; Warshel, A. *J. Phys. Chem. B* **2001**, *105*, 7887.
(62) Siebert, M. R.; Zhang, J.; Addepalli, S. V.; Tantillo, D. J.; Hase, W. L. *J. Am. Chem. Soc.* **2011**, *133*, 8335.
(63) Siebert, M. R.; Manikandan, P.; Sun, R.; Tantillo, D. J.; Hase, W. L. *J. Chem. Theory Comput.* **2012**, *8*, 1212.
(64) Zhao, Y.; Truhlar, D. *Theor. Chem. Acc.* **2008**, *120*, 215.
(65) Hehre, W. J.; Radom, L.; Schleyer, P. v. R.; Pople, J. A. *Ab Initio Molecular Orbital Theory*; John Wiley & Sons: New York, 1986.
(66) Alecu, I. M.; Zheng, J.; Zhao, Y.; Truhlar, D. G. *J. Chem. Theory Comput.* **2010**, *6*, 2872.
(67) Frisch, M. J.; Trucks, G. W.; Schlegel, H. B.; Scuseria, G. E.; Robb, M. A.; Cheeseman, J. R.; Scalmani, G.; Barone, V.; Mennucci, B.; Petersson, G. A.; Nakatsuji, H.; Caricato, M.; Li, X.; Hratchian, H. P.; Izmaylov, A. F.; Bloino, J.; Zheng, G.; Sonnenberg, J. L.; Hada, M.; Ehara, M.; Toyota, K.; Fukuda, R.; Hasegawa, J.; Ishida, M.; Nakajima, T.; Honda, Y.; Kitao, O.; Nakai, H.; Vreven, T.; J. A. Montgomery, J.; Peralta, J. E.; Ogliaro, F.; Bearpark, M.; Heyd, J. J.; Brothers, E.; Kudin, K. N.; Staroverov, V. N.; Kobayashi, R.; Normand, J.; Raghavachari, K.; Rendell, A.; Burant, J. C.; Iyengar, S. S.; Tomasi, J.; Cossi, M.; Rega, N.; Millam, J. M.; Klene, M.; Knox, J. E.; Cross, J. B.; Bakken, V.; Adamo, C.; Jaramillo, J.; Gomperts, R.; Stratmann, R. E.; Yazyev, O.; Austin, A. J.; Cammi, R.; Pomelli, C.; Ochterski, J. W.; Martin, R. L.; Morokuma, K.; Zakrzewski, V. G.; Voth, G. A.; Salvador, P.; Dannenberg, J. J.; Dapprich, S.; Daniels, A. D.; Farkas, O.; Foresman, J. B.; Ortiz, J. V.; Cioslowski, J.; Fox, D. J. *Gaussian 09, revision B.01*; Gaussian, Inc.: Wallingford, CT, 2009.
(68) Torrie, G. M.; Valleau, J. P. *J. Comput. Phys.* **1977**, *23*, 187.
(69) Rajamani, R.; Naidoo, K. J.; Gao, J. *J. Comput. Chem.* **2003**, *24*, 1775.
(70) Doron, D.; Kohen, A.; Major, D. T. *J. Chem. Theory Comput.* **2012**, *8*, 2484.
(71) Brooks, C. L., III; Brünger, A.; Karplus, M. *Biopolymers* **1985**, *24*, 843.
(72) MacKerell, A. D.; Bashford, D.; Bellott, M.; Dunbrack, R. L.; Evanseck, J. D.; Field, M. J.; Fischer, S.; Gao, J.; Guo, H.; Ha, S.; Joseph-McCarthy, D.; Kuchnir, L.; Kuczera, K.; Lau, F. T. K.; Mattos, C.; Michnick, S.; Ngo, T.; Nguyen, D. T.; Prodhom, B.; Reiher, W. E.; Roux, B.; Schlenkrich, M.; Smith, J. C.; Stote, R.; Straub, J.; Watanabe, M.; Wiorkiewicz-Kuczera, J.; Yin, D.; Karplus, M. *J. Phys. Chem. B* **1998**, *102*, 3586.
(73) Jorgensen, W. L.; Chandrasekhar, J.; Madura, J. D.; Impey, R. W.; Klein, M. L. *J. Chem. Phys.* **1983**, *79*, 926.
(74) Azuri, A.; Engel, H.; Doron, D.; Major, D. T. *J. Chem. Theory Comput.* **2011**, *7*, 1273.
(75) Brooks, B. R.; Bruccoleri, R. E.; Olafson, B. D.; States, D. J.; Swaminathan, S.; Karplus, M. *J. Comput. Chem.* **1983**, *4*, 187.
(76) Brooks, B. R.; Brooks, C. L., III; Mackerell, A. D., Jr.; Nilsson, L.; Petrella, R. J.; Roux, B.; Won, Y.; Archontis, G.; Bartels, C.; Boresch, S.; Caflisch, A.; Caves, L.; Cui, Q.; Dinner, A. R.; Feig, M.; Fischer, S.; Gao, J.; Hodoscek, M.; Im, W.; Kuczera, K.; Lazaridis, T.; Ma, J.; Ovchinnikov, V.; Paci, E.; Pastor, R. W.; Post, C. B.; Pu, J. Z.; Schaefer, M.; Tidor, B.; Venable, R. M.; Woodcock, H. L.; Wu, X.; Yang, W.; York, D. M.; Karplus, M. *J. Comput. Chem.* **2009**, *30*, 1545.
(77) Shao, Y.; Fusti-Molnar, L.; Jung, Y.; Kussmann, J.; Ochsenfeld, C.; Brown, S. T.; Gilbert, A. T. B.; Slipchenko, L. V.; Levchenko, S. V.; O'Neill, D. P.; DiStasio, R. A., Jr.; Lochan, R. C.; Wang, T.; Beran, G. J. O.; Besley, N. A.; Herbert, J. M.; Lin, C. Y.; Voorhis, T. V.; Chien, S. H.; Sodt, A.; Steele, R. P.; Rassolov, V. A.; Maslen, P. E.; Korambath, P. P.; Adamson, R. D.; Austin, B.; Baker, J.; Byrd, E. F. C.; Daschel, H.; Doerksen, R. J.; Dreuw, A.; Dunietz, B. D.; Dutoi, A. D.; Furlani, T. R.; Gwaltney, S. R.; Heyden, A.; So, H.; Hsu, C.-P.; Kedziora, G.; Khaliullin, R. Z.; Klunzinger, P.; Lee, A. M.; Lee, M. S.; Liang, W.; Lotan, I.; Nair, N.; Peters, B.; Proynov, E. I.; Pieniazek, P. A.; Rhee, Y. M.; Ritchie, J.; Rosta, E.; Sherrill, C. D.; Simmonett, A. C.; Subotnik, J. E.; Woodcock, H. L., III; Zhang, W.; Bell, A. T.; Chakraborty, A. K.; Chipman, D. M.; Keil, F. J.; Warshel, A.; Hehre, W. J.; Schaefer, H. F., III; Kong, J.; Krylov, A. I.; Gill, P. M. W.; Head-Gordon, M. *Phys. Chem. Chem. Phys.* **2006**, *8*, 3172.